Many-particle effects at core thresholds in simple metals

P. A. Bruhwiler* and S. E. Schnatterly
Jesse Beams Laboratory of Physics, University of Virginia, Charlottesville, Virginia 22903
(Received 3 October 1989)

We have analyzed inelastic electron-scattering (IES) data at the Na $L_{2,3}$ and K $M_{2,3}$ thresholds in terms of the Mahan-Nozières–De Dominicis (MND) model. We have also obtained the absorption coefficient μ and imaginary dielectric function ϵ_2 from the IES data and analyzed them in the same manner as the raw data. For K the peaking parameter α_0 obtained from absorption depends upon whether IES data, μ, or ϵ_2 is used. For Na, α_0 does not vary significantly among the three absorption spectral functions and has a value of 0.22 ± 0.03 if uncertainties in the transition density of states are included. Exchange mixing is found to be a small effect at the Na $L_{2,3}$ absorption edge. We have reanalyzed published p-core soft-x-ray emission data from Na and K and account for the effects of partial phonon relaxation on α_0. In both cases α_0 is significantly less than for the corresponding absorption spectra with values of about 0.15. We have also reanalyzed published Na core-level x-ray photoemission spectroscopy data including surface contributions and for the appropriate exponent obtain $\alpha=0.22\pm0.02$. The results above taken in concert indicate a failure in the presently accepted MND model. We suggest that previously unconsidered dynamical effects must be included.

I. INTRODUCTION

Studies of electronic band structure of metals with the use of soft-x-ray emission had been pioneered by the early 1940s,[1,2] but interpretation of the spectra was limited to one-electron descriptions for a number of years. Some early attempts to improve upon the single-particle picture focused on the low-energy tail:[3,4] the theory of that feature has recently been advanced to give a semiquantitative understanding.[5,6] The other prominent many-body structure in x-ray spectra of metals is the well-known peaking at p-core thresholds in absorption and emission. Mahan was able to account for the peaking as an excitonic effect,[7] but did not include the suppression at threshold which is due to the many-body overlap integral discussed by Anderson.[8] Nozières and De Dominicis developed a model[9] incorporating both effects that is valid asymptotically close to threshold, i.e., in the limit of the long-time response. Their result has become known as the Mahan-Nozières–De Dominicis (MND) model.[10]

The MND expression for the spectral intensity at an x-ray absorption threshold is

$$I(E)\propto\sum_{l=0}^{\infty}A_l(E)\left[\frac{\zeta}{E-E_T}\right]^{\alpha_l}\Theta(E-E_T)\ , \tag{1}$$

where the $A_l(E)$ are the dipole transition-matrix elements, ζ is a scaling parameter on the order of the Fermi energy (E_F), and E_T is the threshold energy. α_l is given by

$$\alpha_l\equiv\frac{2\delta_l}{\pi}-\alpha\ , \tag{2}$$

$$\alpha\equiv2\sum_{l=0}^{\infty}(2l+1)\left[\frac{\delta_l}{\pi}\right]^2\ . \tag{3}$$

The δ_l are the phase-shift changes at E_F for single-particle conduction states of angular momentum l, evaluated using the initial and final potentials. In this paper we are considering p-core spectra: the dipole rule thus selects only $l=0$ and $l=2$ components of the density of states (DOS), and $l=2$ contributions can be neglected for the cases considered.[11,12,10] Hence α_0 is expected to characterize the spectra essentially completely.

Much effort has been invested in attempts to understand aspects of the validity and applicability of MND theory. When Doniach and Šunjić showed that α [Eq. (3)] can be measured in x-ray photoemission (XPS) core spectra,[13] the stage was set for the comprehensive studies which have been carried out through the last 15 years.[10] The goals of those studies can be divided roughly into the following three areas: (1) Determination of the range of energy beginning at E_T (or E_F) to which the asymptotic MND theory can be applied quantitatively to data; (2) The effects of the one-electron DOS structure, phonon coupling to the core hole, core lifetime, etc.[10] on the values of the α_l determined from experiment; (3) Self-consistency checks—do absorption data provide a picture consistent with the available emission and XPS spectra?

Many of the early investigations focused on the phonon broadening[14,15] and lifetime broadening[15] of the core state. The transition DOS (TDOS) was considered at about the same time (see, e.g., Ref. 16) and incorporated into soft-x-ray absorption (SXA) and emission (SXE) line-shape analyses soon thereafter.[17,12] Attempts to theoretically define the regime in which the MND model is quantitatively valid led to results which were seen as very restrictive[18] and alternately to results which gave support to applicability of the power law far away from threshold.[19] Experimentalists[17] have made apparently arbitrary and even inconsistent[12,20] choices in this regard.

We have recently shown[21] using a determinantal method[6,5] and a realistic free-electron DOS, that for Na a range of 0.5 eV from threshold gives accurate exponents, even though the results also indicated a slight inherent asymmetry between absorption and emission. As shown below, it is important to be able to avoid complete reliance on the first 0.2 eV or so from threshold for fitting data, since the broadening influences dominate the spectral shape in that region.

Consistency between XPS and SXA data remains as a definitive test of the quantitative validity of the MND model. Much the same can be said for the experimental efforts, with only one group claiming to have shown for example that the Na SXA data are consistent with the XPS results.[12] There is therefore much left to be understood about the validity of the MND model in describing real spectra.

We have taken advantage of the ability of inelastic electron scattering (IES) experiments to measure absorption over a wide range to perform Kramers-Kronig analyses of K $M_{2,3}$ and Na $L_{2,3}$ threshold data which have been presented previously.[17] We obtain and compare for both metals the imaginary part of the dielectric constant ϵ_2, the absorption coefficient μ, and $\mathrm{Im}(-1/\epsilon)$, the first of which can be compared directly with calculations, and the latter two measured.[23] We find that the choice of spectral function one considers has little bearing on the values of the broadening parameters extracted in fits. The peaking parameter α_0 varies significantly among the three response functions in the case of the K $M_{2,3}$ edge though negligibly for the Na $L_{2,3}$ threshold.

We have also investigated the role of partial phonon relaxation broadening[24,25] on the Na $L_{2,3}$ emission shape and find that it cannot account for the differences in threshold peaking between the emission and absorption spectra: this result was first noted in earlier work.[26] In addition we discuss how close to threshold a model can be used to distinguish between different values of α_0 in data. Finally, we investigate and discuss the possible influence of surface effects[27-29] on the XPS data analysis.[15]

II. DETERMINATION OF THE ABSORPTION RESPONSE FUNCTION

IES measurements, which can be obtained over a relatively large energy range,[23] enable one to determine the optical properties of a material through a Kramers-Kronig analysis. All previous analyses of absorption experiments have used either $\mu(E)$ or $\mathrm{Im}[-1/\epsilon(E)]$, whereas the quantity evaluated using the MND model is $\epsilon_2(E)$. Thus several steps must be undertaken before fitting any line shape to the data. Confident multiple-scattering removal[30,6,23] must be performed in order to determine the true $\mathrm{Im}[-1/\epsilon(E)]$. After Kramers-Kronig analysis to obtain μ and ϵ_2, it is necessary to remove the background due to valence contributions[23] which varies roughly as $1/E^3$. The importance of removing this background is apparent when fitting a line shape to the data, and is discussed further in Secs. III and IV.

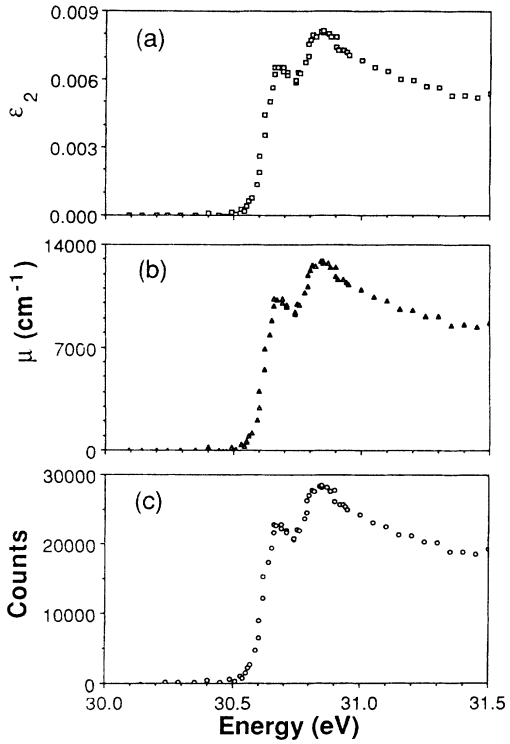

FIG. 1. Na $L_{2,3}$ response functions at threshold. (a) and (b) are given in proper units, and $\mathrm{Im}(-1/\epsilon)$ is given in shape by the raw IES data in (c).

After carrying out the multiple-scattering correction and Kramers-Kronig analysis for Na and K data[17] over the energy range 0–100 eV we obtained $\mu(E)$, $\epsilon_2(E)$, and $\mathrm{Im}[-1/\epsilon(E)]$ in the Na $L_{2,3}$ and K $M_{2,3}$ threshold regions shown in Figs. 1 and 2, respectively. In the case of

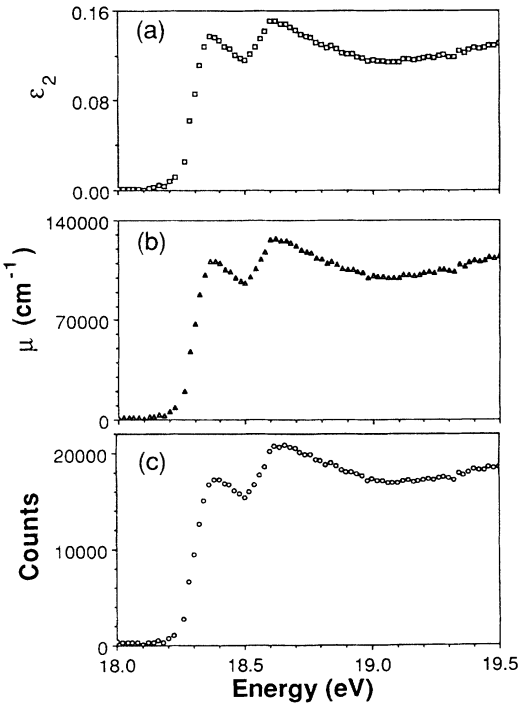

FIG. 2. The same as Fig. 1, for the K $M_{2,3}$ threshold.

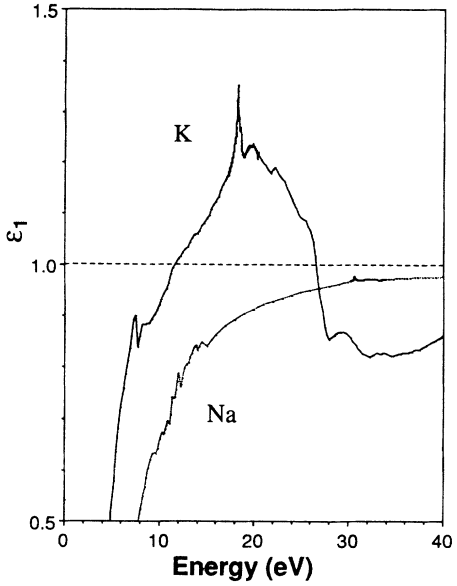

FIG. 3. ϵ_1 for Na and K, indicating the large derivatives at threshold of the transitions discussed in the text.

Na the region between 15 and 30 eV and above 34 eV was not measured, but was approximated based on other measurements,[31–33] and the Kramers-Kronig evaluation should give reasonable results in the narrow threshold region. The results for $\mu(E)$ in both cases are comparable to the optical measurements.[33,34] As a means of comparison we take the magnitude of the rise in $\mu(E)$ at threshold an find approximate ratios of 1.5 (0.8) for IES-derived results divided by optical values for Na (K). This agreement seems good considering the fact that the optical line shapes vary somewhat between the two studies which have been published.[34,33] Our analysis also yields $\epsilon_1(E)$. For Na, $\epsilon_1(E)$ is insensitive to rather large variations in the choice of data we patch to our threshold data for the Kramers-Kronig analysis. We show $\epsilon_1(E)$ for both metals in Fig. 3 and compare to the value of 1.0 expected at high energies. In the case of Na we see a deviation of about 0.05 at threshold, while for K the difference is near 0.40. It is these deviations which are related to the differences between $\epsilon_2(E)$, $\mu(E)$, and $\mathrm{Im}[-1/\epsilon(E)]$. The effects signified by this structure in $\epsilon_1(E)$ are analyzed in greater detail in Sec. IV.

III. LINE-SHAPE ANALYSIS

A. Absorption and emission thresholds

Once the background has been properly subtracted from the data, the MND line shape may be fitted. We find that over the short energy range (about 2 eV) needing background removal a linear background is no different from one which varies as $1/E^3$. Our model is simply the MND power law applied to a model TDOS, and then broadened appropriately to account for the finite core lifetime, Fermi statistics, phonons, and instrumental effects. The model spectral function $F(E)$ can be expressed as follows:

$$F(E)=Af(E-E_T)+Bf(E-(E_T+\Delta)) , \tag{4}$$

$$f(E)=\int_{-\infty}^{\infty}\frac{dE_1}{\sqrt{(2\pi)}\sigma}\exp\left[\frac{-(E-E_1)^2}{2\sigma^2}\right]\int_{-\infty}^{\infty}\frac{dE_2}{kT}\frac{1}{2+\exp[(E_1-E_2)/kT]+\exp[(E_2-E_1)/kT]}$$
$$\times\int_{-\infty}^{\infty}\frac{dE_3}{\pi}\frac{\gamma/2}{(E_2-E_3)+(\gamma/2)^2}\Theta(E_3)E_3^{-\alpha_0}(1-mE_3) , \tag{5}$$

where A is the L_3 amplitude, B is the L_2 amplitude, Δ is the spin-orbit splitting, E_T is the threshold energy, m equals the ratio of DOS slope to DOS amplitude at E_F (i.e., E_T), α_0 is the threshold exponent, γ is the Lorentzian full width at half maximum (FWHM) corresponding to the core lifetime,[35] and 2.36σ is the Gaussian FWHM.

The integral over E_3 was performed analytically to contour integration,[26] and can be broken into two parts: the convolution of a Lorentzian with (a) a step function and (b) a step function multiplied by a line passing through the origin, both of which have been modified by the MND peaking. The result of (a) is the Doniach-Šunjić (DS) function,[13] although calculated in a different way; (b) provides the following similar function:

$$I_{LS}(E,\gamma,\alpha_0,m)=m[E^2-(\gamma/2)^2]^{(1-\alpha_0)/2}\times\frac{\cos\frac{\pi\alpha_0}{2}+(1-\alpha_0)\tan^{-1}\left[\frac{2E}{\gamma}\right]}{\sin(\pi\alpha_0)} . \tag{6}$$

In these terms, the DS function is

$$I_S(E,\gamma,\alpha_0)=[E^2+(\gamma/2)^2]^{-\alpha_0/2}\times\frac{\cos\frac{\pi}{2}(1-\alpha_0)+\alpha_0\tan^{-1}\left[\frac{2E}{\gamma}\right]}{\sin(\pi\alpha_0)} . \tag{7}$$

Since the Na TDOS has been calculated[16,12,11] we can include the slope of that function near threshold and thereby account reasonably well for the deviation from a pure step function. Though the integrals over E_1 and E_2 are easily optimized due to the nonsingular nature and rapid decay of their integrands, it is quite important that we can carry out the lifetime broadening analytically. We thereby avoid errors of earlier work[17] due to the numerical evaluation of a singular integral. Comparison of analytical [Eq. (7)] to numerical results of the E_3 integral in Eq. (5) shows that the broadening is underestimated immediately below threshold and the peaking at threshold is overestimated by numerical evaluation. We have taken extreme measures in attempts to improve numerical approximations of this integral, letting step sizes vary over 30 orders of magnitude and extending the upper integration limit far above the point needed for convergence to a unique result. We nevertheless find that simple methods such as Simpson's rule are inadequate, and that the analytical result must be employed to obtain the needed accuracy near threshold. For energies on the order of 0.1 eV and further away from threshold in both directions the two results are equivalent. It was this inadequacy of the numerical integration which resulted[17] in an underestimate of the $2p$-core lifetime broadening Na of $\gamma=23$ meV. Our present result is $\gamma=4\pm2$ meV, in excellent agreement with recent theoretical estimates.[35]

There have been indications[37–39] that simply convoluting the line-shape model with the derivative of the Fermi-Dirac function is not appropriate to take the finite temperature of the electron gas into account. The usual Fermi-Dirac broadening is given by the convolution function in the integral over E_2 in Eq. (5). This function is nearly Gaussian with a second moment

$$\sigma_{\mathrm{FD}}^2=(\pi kT)^2/3 \ . \tag{8}$$

The closed-form theoretical result[37,38] in the presence of the MND many-body effect is

$$\sigma_{\mathrm{FD-MND}}^2=(1-\alpha_0)\sigma_{FD}^2 \tag{9}$$

which gives substantially less broadening with typical values of α_0 for p-core thresholds. Since second moments of Gaussians add in convolutions, it is a simple matter to convert results obtained with one expression to those which would be found using the other assuming that other broadening sources are large enough. We note that the Fermi-Dirac derivative function has tails which extend beyond those of a Gaussian with the same second moment, which means that use of a Gaussian to approximate its effects may not be accurate when other broadening effects are of comparable or lesser magnitude. The extracted MND line-shape parameters do not depend on which algorithm is chosen to describe this temperature effect, though the phonon broadening parameters can be significantly affected.

Several groups have previously analyzed Na $L_{2,3}$ absorption data,[32,17,12,40] and at least two[17,12] have carefully considered the effects of exchange mixing[40,10] which causes the L_3/L_2 intensity ratio to deviate from the L-S coupling value of 2. We reconsider this effect for Na in Sec. IV. In general,[41] if a p-core absorption spin-orbit intensity ratio is not 2, then the line shape developed by Onodera[40] or Almbladh and Hedin[10] must be substituted for the pair of functions described above in Eqs. (6) and (7). We reiterate, however, that for a proper determination of the intensity ratio a Kramers-Kronig analysis and background subtraction must be carried out.

Onodera's expression for the line-shape presence of exchange mixing is as follows:

$$[I(E)]_{\mathrm{Onodera}} \propto \mathrm{Im}\left[\frac{2R(E)+R(E-\Delta)}{3+3K[2R(E)+R(E-\Delta)]}\right] \tag{10}$$

with

$$R(E)=\frac{(E_T-E)^{\alpha_0}-1}{-\sin\pi\alpha_0} \ , \tag{11}$$

where Δ is the spin-orbit splitting as in Eq. (4) and K parameterizes the strength of the exchange mixing.[17,40,10] As we have indicated above, it is important to include lifetime broadening analytically in the absence of an accurate numerical method. Onodera's prescription for this is to add an imaginary part to E corresponding to the core lifetime, i.e., $E\rightarrow E-i\gamma/2$. To compare this method to the exact result [Eq. (7)] we set $K=0$ in Eq. (10), which then reduces to

$$[I(E;K=0,\gamma\neq0)]_{\mathrm{Onodera}} \propto [2R_I(E-i\gamma/2)+R_I(E-i\gamma/2-\Delta)]/3 \ , \tag{12}$$

where

$$R_1(E-i\gamma/2)=\frac{\sin\left[\alpha_0\tan^{-1}\left[\frac{-\gamma}{-2E}\right]\right]}{[E^2+(\gamma/2)^2]^{\alpha_0/2}} \ . \tag{13}$$

This function is equivalent to that in Eq. (7). A difficulty which remains is how to properly include TDOS variations in the full Onodera line shape.

A further complication which has been discussed at length by Fink *et al.*[28] (hereafter referred to as FFF) is the anomalous L_3/L_2 intensity ratio found in many SXE spectra (see also Crisp, Ref. 41) which varies from about 6 in Na to more than 60 in Cs. The total lifetime of the L_2 component was found to be shortened compared to that of the L_3 component in the heavy alkali metals due to Coster-Kronig transitions.[28] While a difference between the Auger transition rates should strongly influence the emission intensity ratio, causing experimentally observed[42,32,28] changes from the expected statistical value of 2, the absorption intensity ratio is influence by the ratio of the *radiative* transition rates. Nevertheless, different lifetimes for each component should be included in the model based[28] on the emission intensity ratio and L_3/L_2 ionization cross-section ratio. The effect of this is discussed in Sec. IV.

As noted above, the choice of energy range over which the data are to be fitted has appeared to be quite an arbitrary one in the past (see, e.g., Refs. 17 and 21 and references therein). von Barth and Grossmann provided solid

theoretical evidence that, aside from uncertainties about the TDOS, the MND power law should hold quite well for emission over ranges typically used in data analysis.[19] We have confirmed this for absorption as well,[21] using a free-electron DOS. Recently Kita[42] found that deviations from the original result[9] occur quite naturally within the MND framework when less singular terms in the expansion of the response function are included. Yet an examination of those results [see Fig. 1(a) in Ref. 42] for a potential appropriate for Na indicates that the deviations within 0.5 eV or so of threshold could account for no more than about 20% of the difference noted between absorption and emission spectra of Na. Confronted with these theoretical developments and with the ability of the MND power law to describe experimental data well away from the threshold, we were led to propose the inclusion of other dynamical aspects of x-ray transitions in the MND model.[21]

We will also show in Sec. IV that the fitting range when the TDOS is linearly or at least slowly varying must be on the order of 0.5 eV to enable a unique determination of α_0. If the TDOS varies rapidly with a large curvature or if the fitting range is too small, ambiguities in the parameters extracted are unavoidable. In the case of the prototypical simple metal Na the broadening effects dominate the spectrum near threshold and can mask deficiencies in a fit to the data in this range. Thus the several tenths of an eV above the L_2 peak in Na represent the experimentally accessible region in determinations of peaking exponents.

B. X-ray photoemission thresholds

The analysis of XPS core line shapes in terms of the MND model was stimulated by DS (Ref. 13) and carried out soon thereafter[15] for several simple metals. It was found that the DS function described the measured line shape excellently over an energy range on the order of $E_F/2$ in every case, and different core levels gave the same value of α as well. Since several calculations of α agreed with the empirical results, this was taken as direct confirmation of MND theory and as the foundation for analysis of other spectra.[12,20]

With the discovery[27] of a significant surface-atom core-level shift (SCS) in Na a reanalysis of the XPS data[15] was needed, since the surface contribution is expected to range from about 15% to 50% for different core levels in the available data. Citrin *et al.*[29] found that the surface and bulk core line shapes were identical within experimental uncertainties for Au, and that only the outer surface layer of atoms possessed a SCS. Kammerer *et al.*[27] made use of those assumptions to evaluate the SCS of Na. Therefore we also adopt the view[29,27] that the same α can to a first approximation describe both surface and bulk contributions to a given spectrum. Hence our line shape consists of the one DS function per bulk core level, with a SCS "partner" DS function scaled in intensity and shifted according to the results of Kammerer *et al.* Using Fig. 4 in Ref. 27 we assign intensities of 15%, 15%, and 48% relative to the bulk to the surface components of the Na $2p$, $2s$, and $1s$ lines, respectively, based on the photon energy used to acquire the data.[15]

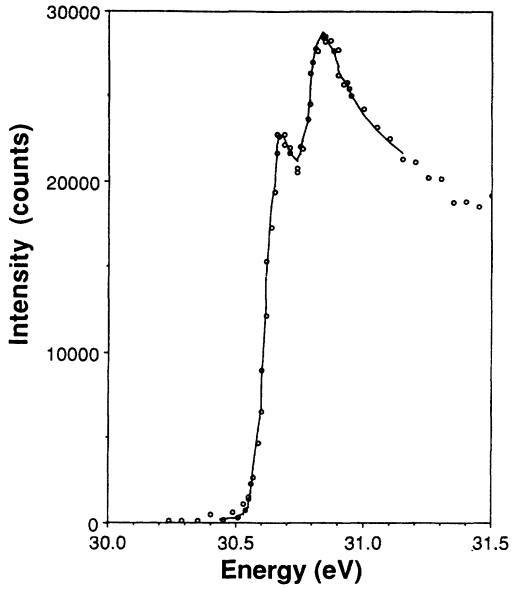

FIG. 4. Fit to Na $L_{2,3}$ IES data using MND line shape with no TDOS slope.

IV. RESULTS AND DISCUSSION

A. Absorption thresholds

A typical fit to Na IES data is shown in Fig. 4. We have used two DS functions with an amplitude ratio of 1.95, $\alpha_0=0.24$, and $\gamma=4$ meV. The total Gaussian broadening is given by $\sigma \simeq 32$ meV. This fit achieved the minimum χ^2 with this fitting range. With γ held fixed we find the χ^2 versus dependence given in Fig. 5 for various fitting ranges. The behavior shown there is typical of all of our line-shape analyses and indicates that fitting up to 31.2 eV, or about 0.6 eV above the $p_{3/2}$ threshold, pro-

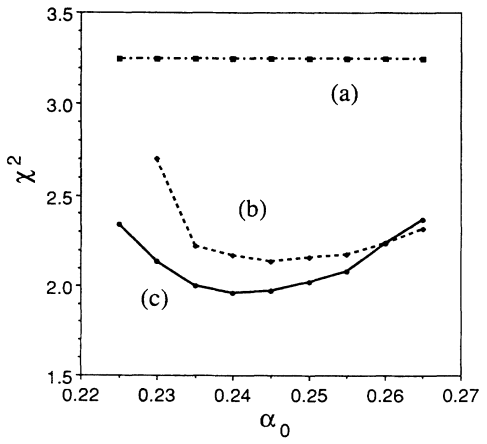

FIG. 5. χ^2 fits to the data in Fig. 4, as α_0 and the fitting range are varied. The ranges represented are 30.4 eV to (a) 30.7 eV, (b) 31.1 eV, and (c) 31.2 eV.

vides unique results. Much shorter ranges yield ambiguous results and much longer ranges require inclusion of a TDOS with nonmonotonic structure.

As noted by Slusky *et al.*,[17] the *s*-like DOS of Na calculated by Gupta and Freeman[16] has an approximate slope above threshold of -0.2 eV^{-1}, assuming unit height at E_F. The (s,d)-like TDOS calculation of Citrin *et al.*[12] (CWS) is nearly the same in this regard. Unfortunately both calculations relied on wave functions generated with the ground-state potential in violation of the final-state rule[19,11,5] (FSR) for absorption, though FSR compatible for SXE. von Barth and Grossman have calculated the Na TDOS and matrix elements for both emission and absorption.[11] Using a repeated-cluster method they obtained realistic results and found that the *d*-like TDOS makes a negligible contribution to the spectra. The normalized slope of the *s*-like TDOS above threshold from their figures is about -0.26 eV^{-1}, about 20% steeper than that of Gupta and Freeman. However, the TDOS slope below E_F which they obtain is close to -0.16 eV^{-1}, which is more than twice the value indicated by the FSR-compatible calculations of the other two groups, -0.04 and -0.07 eV^{-1}. It is therefore not clear how to gauge the accuracy of these calculations. We take -0.20 eV^{-1} and -0.10 eV^{-1} to be reasonable upper limits on the theoretical TDOS slopes for absorption and emission, respectively. Upon including a TDOS slope of -0.2 eV^{-1} in our model we find that α_0 decreases from 0.24 to 0.19. If we let the slope m vary freely the best fit is obtained when $\alpha_0=0.22\pm0.01$ and $m\simeq-0.07$, in close agreement with earlier results.[17] We thus have three results for α_0 using three slopes, and find that $\alpha_0\simeq0.25m+0.24$ describes the trend in the Na $L_{2,3}$ absorption spectra for this range of values of m. These results, as well as the results for the K $M_{2,3}$ spectra, are summarized in Table I for analysis with $m=0$.

In Fig. 6 we show the data of Haensel *et al.*[31] before and after removal of the background estimated from the short interval below threshold, and compare the latter to our estimate of $\mu(E)$. The agreement is good, and would perhaps be improved if the background were accurately known. Upon fitting those data using $\gamma=4$ meV we find the results shown in Table I with a best-fit Gaussian of $\sigma\simeq29$ meV. Our intensity ratios and threshold exponents follow fairly closely those obtained in earlier

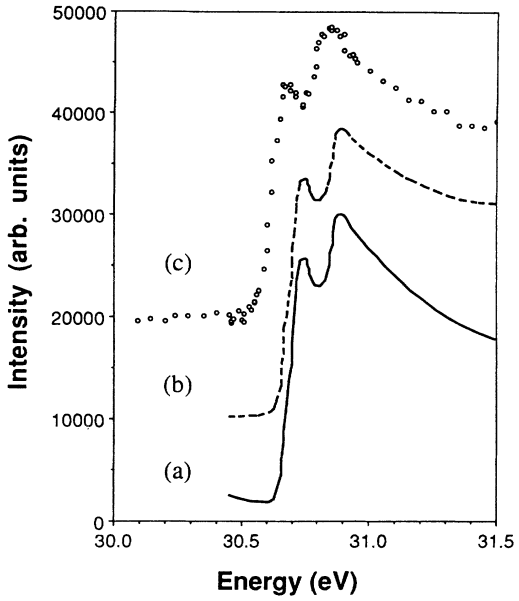

FIG. 6. The Na $L_{2,3}$ absorption data of Ref. 31 (a) before and (b) after removing a background determined using the slope of the data [(a)] at 30.5 eV. Also shown (c) are the IES data. A calibration difference is apparent between (b) and (c).

work,[17] with the exception that $\mu(E)$ and $\epsilon_2(E)$ were not investigated at that time. The good agreement between our results using the IES data and using the data of Haensel *et al.* indicates that the choice of spectral function does not significantly affect the results of a MND line-shape analysis for Na, unlike the case for K. The parameters given in Table I reinforce this conclusion.[43]

The fact that the intensity ratio is so close to 2 for the Na data presented here indicates[10] that exchange mixing is insignificant at the Na $L_{2,3}$ absorption threshold, in contrast to the theoretical findings[10] and the data analysis of CWS. It is noteworthy that some previous workers have estimated the intensity ratio simply on the basis of the amplitudes at the peak maxima. When considering peaked functions such as implied by the MND power law, it would seem apparent *a priori* that such an approach is prone to error.

As noted in Sec. III A, the $p_{1/2}$-core lifetime broaden-

TABLE I. Fitting parameters for absorption spectral functions using a step-function TDOS.

Threshold	Spectral function	Spin-orbit ratio	α_0	T (K)
	$\mathrm{Im}(-1/\epsilon)$	2.50	0.16±0.01	
K $M_{2,3}$	μ	2.56	0.21±0.01	208
	ϵ_2	2.62	0.24±0.01	
	$\mathrm{Im}(-I/\epsilon)$	1.95	0.24±0.01	
Na $L_{2,3}$	μ	1.84	0.24±0.01	112
	ϵ_2	1.91	0.24±0.01	
Na $L_{2,3}$ (Data of Ref. 31)	μ	2.05	0.205±0.01	77

ing is greater than that of the $p_{3/2}$ core due to Coster-Kronig Auger processes.[28] Since the absorption intensity ratio is 2, and the emission intensity ratio is about 7, using the results of Ref. 28 we find that for Na the ratio of Auger lifetime widths $\gamma_{1/2}/\gamma_{3/2}$ is $\frac{8}{3}$. While this difference has no effect on the value of $\gamma_{3/2}$ which corresponds to the lowest χ^2 in fits to the data ($\gamma_{3/2}=4$ meV), inclusion of the larger $\gamma_{1/2}$ results in a slightly lower χ^2. Other parameters are unaffected.

In Table I we see again that the K $M_{2,3}$ edge is highly dependent on the probe chosen to measure it. Though the spin-orbit ratio is fairly constant, α_0 varies from 0.16 to 0.24. Thus $\epsilon_1(E)-1$ has a dramatic effect on the peaking behavior detected experimentally. The reason that $\epsilon_1(E)-1$ is large stems from the fact that the $M_{2,3}$ threshold is low lying in energy, so that the dipole matrix element near threshold is large. This pattern should be followed by the heavier alkalis Rb and Cs as well, and exposes the need for further theoretical work to make contact between our results and the MND framework. It seems to us that ϵ_2 is the preferred response function to compare to calculations and other data when the three differ in shape. However, it is not clear that the MND model should even be expected to be accurate in cases where this difficulty exists. We found that we could not confidently determine γ or the phonon broadening of the K spectra.

The peaking parameter for $\mu(E)$ at the K $M_{2,3}$ edge cited by Miyahara *et al.*[44] is $\alpha_0=0.28\pm0.02$. Apparently this value was obtained by taking the logarithm of Eq. (1) and evaluating the slope,[34] equating it to α_0. However, this algorithm requires an accurate knowledge of the threshold energy, which must be subtracted from the abscissa of the raw data. Ishii *et al.*[34] chose to use the midpoint of the rise at threshold as the placement of E_T. As has been shown,[32] though, lifetime and thermal broadening shift the midpoint of the threshold away from E_T to lower energies when α_0 is positive. Thus the Ishii algorithm is equivalent to evaluating the slope of $-\alpha_0\ln[E-(E_0+\epsilon)]$ versus $\ln(E-E_0)$, where the threshold midpoint position is $E_0=E_T-\epsilon$. We therefore disagree with Miyahara *et al.* that this method tends to give lower limits on α_0. A valid comparison of our results to theirs must await reanalysis of their data.

B. Emission thresholds

Both Na $L_{2,3}$ and K $M_{2,3}$ emission spectra have been studied by various workers recently.[41,32,44–46] Crisp[41,45] and FFF (Refs. 46 and 28) have each carefully investigated the effects of self-absorption[47] on the spectra and successfully eliminated them in the threshold region. This is quite important for estimating the broadening factors and to remove serious doubts about the influence of self-absorption on the apparent value of α_0.

We have compared Crisp's low-temperature Na $L_{2,3}$ SXE data[41] with those of Callcott *et al.*[32] and find that they agree quite closely, except for a slight suppression due to self-absorption evident in the data of Callcott *et al.* above threshold. Crisp eliminated the effects of self-absorption by going to low-energy excitation, and found he could also correct data measured with high-energy excitation.[41] We have analyzed Crisp's Na data with our line-shape model, using the value of γ obtained from analysis of the IES data (see Table I), $\gamma=4$ meV. Analysis of emission data is complicated by partial phonon relaxation,[24,25] the effects of which have been quite firmly established.[48–50] Using Mahan's formalism[24] we have investigated the phonon broadening shape which one should expect to be evident in Na $L_{2,3}$ spectra. The parameters which must be supplied to the Mahan model are the phonon frequency (ω), relaxation rate (Γ), and coupling constant[51] (S), the core width γ, and the temperature. We obtain both the absorption and emission broadening shapes. By calculating the first moment of each we find the theoretical Stokes shift.[24,25] Since the Stokes shift[32] and phonon broadening are known within experimental uncertainties, we can impose needed constraints on the model, which is capable of generating many different broadening profiles.

The absorption broadening line shape is determined almost entirely[24,25,48] by S and ω, although Γ exerts a small influence. Thus temperature-dependent absorption data can be evaluated using the following expression to determine S and ω:[51]

$$\sigma_{\rm pho}^2=S(\hbar\omega)^2\coth\frac{\hbar\omega}{2kT}\ , \tag{14}$$

where $\sigma_{\rm pho}^2$ is the Gaussian broadening due to phonons. Since we also obtain γ from the absorption data there is only one free parameter in the Mahan model, to the extent that experimental uncertainties in the other four parameters are small. We are implicitly assuming that linear phonon coupling to one phonon mode is an adequate description,[51] which has recently received some theoretical justification[52] in the case of Na, as well as experimental support for the heavier alkali metals.[28] If we assume that the breathing mode of Na, $\hbar\omega\simeq10$ meV (Ref. 53), is the effective mode for the problem, however, we find that the model does not produce the correct Stokes shift for any value of Γ. Choosing $\hbar\omega=13$ meV allows much better agreement if $\Gamma\simeq\omega$. Typical broadening shapes are given in Fig. 7, and are seen to be not far from Gaussian for emission as well as absorption. Thus the tactic of parametrizing SXE phonon broadening by Gaussians seems reasonable in cases like Na and K, for which the phonon and lifetime data should lead to similar predictions within the Mahan model of phonon broadening. A typical fit to Crisp's data is displayed in Fig. 8.

A peculiar feature in the Na SXE spectra is the presence 0.4 eV above threshold of a minimum in intensity, shown from our own measurement at about 300 K in Fig. 9. We have eliminated instrumental effects and self-absorption as possible causes, and have learned that the feature has been measured elsewhere.[54] One implication is that this effect could be influencing the measured Stokes shift or apparent emission edge broadening, as it has the appearance of a Fano resonance.[55,56] Such a minimum has not been observed in any other alkali metal p-core spectra[57] which are expected to be similar to Na. One feature which distinguishes Na from the heavy al-

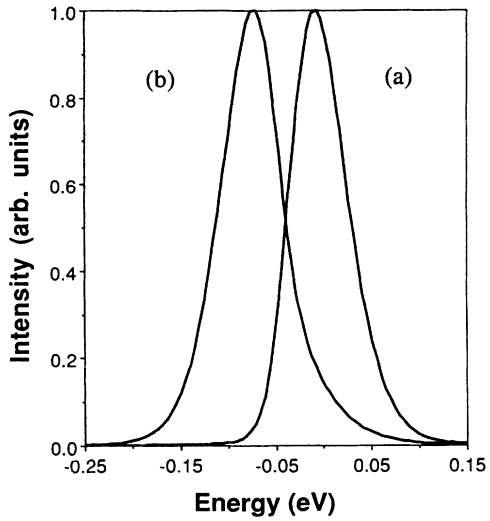

FIG. 7. Representative phonon broadening functions of Na (a) absorption and (b) emission spectra, calculated using Mahan's model of partial phonon relaxation with $\omega=13$ meV, $\Gamma=13$ meV, $\gamma=4$ meV, $S=3.2$, and $T=112$ K.

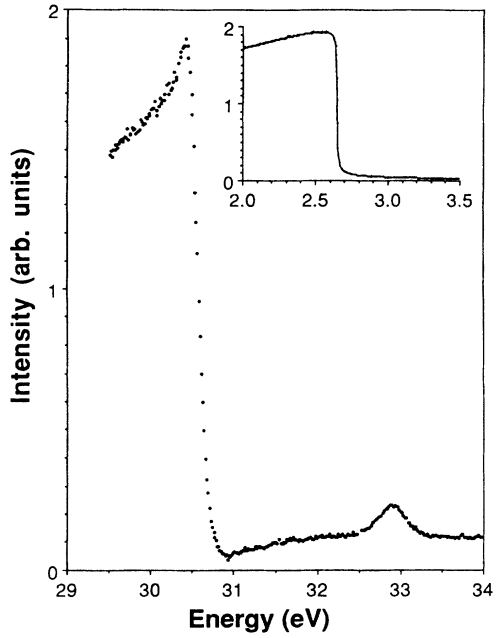

FIG. 9. Na $L_{2,3}$ emission spectrum, showing minimum above threshold and core-core transition at 33 eV, taken at ~300 K.

kalis is the location of the p-core–to–s-core line associated with the p-core emission spectrum, visible for Na in Fig. 9 at 33 eV. For K, Rb, and Cs this peak is expected[58] to lie somewhere within the same energy span occupied by the conduction-band emission. Interestingly no core-core emission is apparent in the spectra of FFF,[28] indicating little or no intensity for that peak in all the heavy alkali metals. We await further investigation of this problem.

We have also analyzed the K $M_{2,3}$ emission data of Crisp[41] and FFF.[28] We choose $\gamma=10$ meV, the value obtained by FFF, assume Gaussian phonon broadening, and find the preliminary result $\alpha_0=0.14\pm0.03$. This is close to the result obtained by Crisp.[41] The TDOS and matrix elements for K have not been studied to our knowledge except for the work of Papaconstantopoulos.[59] He finds that the s-like DOS for all three heavy alkali metals is positively sloped near E_F when calculated in the absence of the core hole. It seems likely then that the difference in peaking between outer p-core absorption and emission spectra of the heavy alkalis, apparent upon a visual inspection, will be substantiated when it becomes possible to fully analyze the data with the MND model.

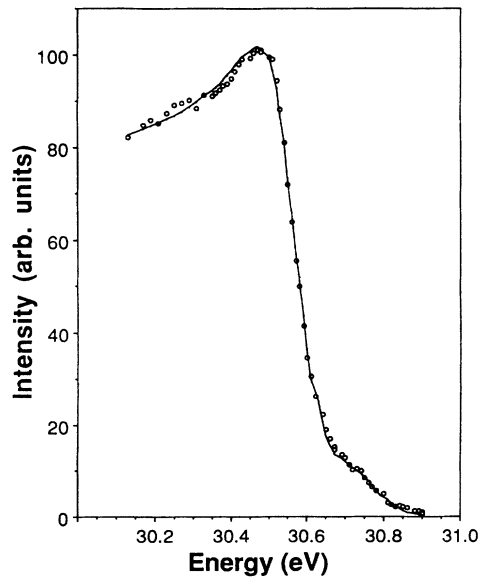

FIG. 8. Typical fit of the MND line shape to the Na emission data of Ref. 43. Data below ≃30.3 eV are from Ref. 32.

C. X-ray photoemission from Na

The best Na XPS data presently available are those of Citrin *et al.*[15] As noted in Sec. III, we model those data with two components per core level, a bulk DS shape, and a surface counterpart shifted to higher binding energy by 0.22 eV. However, unlike Kammerer *et al.*[27] we did not find it necessary to use an artificially low spin-orbit splitting for the $2p$ level, though we could vary the splitting from 0.17 to 0.16 eV with little effect on the results.

In Fig. 10 we show a typical fit to the XPS data, and in Fig. 11 a graph of χ^2 versus α, for different energy ranges. We have estimated χ^2 by assuming the uncertainty in a signal of N counts is given by $\sqrt{N}$. We summarize the present results in Table II, along with the earlier results of Citrin *et al.*[15] As is immediately apparent, very little change in α was required to achieve a good fit after including surface contributions in each case. We have therefore confirmed the earlier detailed analysis,[15] with a revised determination of α only slightly larger than be-

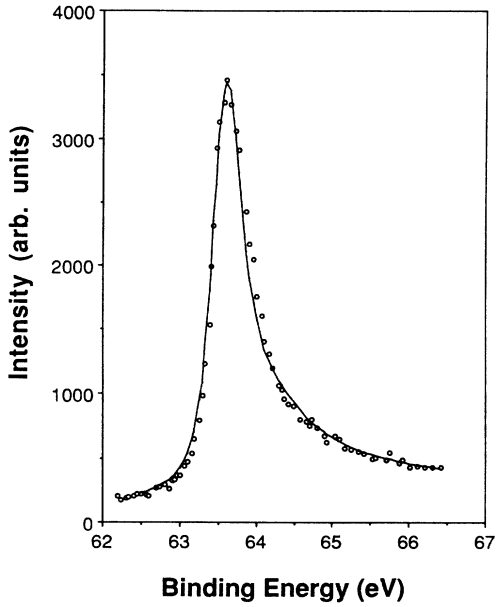

FIG. 10. Typical fit to Na 2*s* XPS data of Ref. 15 using the model described in the text.

fore. The results in Fig. 11 parallel to a large degree those in Fig. 5, providing evidence of the dominance of broadening factors near threshold common to both SXA and XPS.

D. Phase-shift compatibility among SXE, SXA, and XPS

To summarize our results on Na, we have found $(\alpha_0)_{\mathrm{SXE}}=0.15$, $(\alpha_0)_{\mathrm{SXA}}=0.22$, and $\alpha=0.22$. The disparity between emission and absorption is large, and signifies a flaw in our present understanding of the threshold anomaly.

As we have noted elsewhere,[21] a difference between absorption and emission in the present asymptotic model implies a change in the potential near the core between

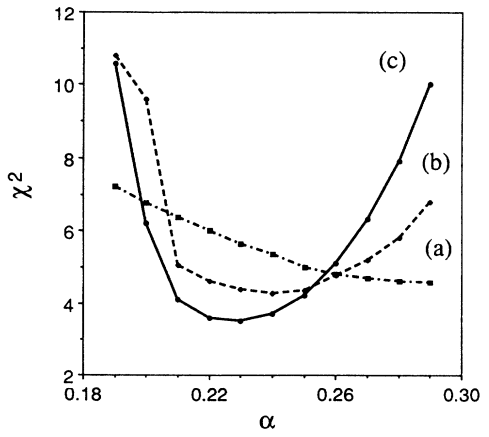

FIG. 11. χ^2 fits to the data in Fig. 10, as a function of α and the fitting range. Fitting ranges shown are 62.5 eV to (a) 64.0 eV, (b) 64.5 eV, and (c) 65.5 eV.

TABLE II. Singularity index for Na XPS core levels.

Core level	α (Present work)	α (Ref. 15)
2*p*	0.22±0.01	0.198±0.015
2*s*	0.23±0.01	0.205±0.015
1*s*	0.22±0.01	0.210±0.015

the two events. Such a change can occur, due to phonon coupling. The absorption transition takes place with the nearby ions in their ground-state equilibrium positions, while the emission transition usually occurs after the nearby ions have relaxed to new positions in the presence of the core potential. Therefore the potential that is switched off in the emission transition will usually be different from that switched on in the absorption transition.

We have shown[26] that in the linear phonon coupling approximation the second moment of the SXA edge broadening due to phonons can be directly related to the charge-density fluctuation at the core. Using the Debye model to sum over frequencies, we obtained $\sigma \simeq (260\ \mathrm{meV})(\Delta\rho/\rho_0)_{\mathrm{rms}}$ for Na, where σ describes the Gaussian phonon broadening, ρ_0 is the average electronic density, and the density ratio is the root-mean-square density fluctuation. The observed[32] Stokes shift of 75 meV for Na implies a density change $\Delta\rho/\rho_0 \simeq 0.29$. The local screening length is then reduced due to this increase in ρ_0, and in the Thomas-Fermi approximation we have found[21] that α_0 decreases by 0.03 using parameters appropriate to Na. While this change is not insignificant, and would perhaps be revised upward by more sophisticated calculations, at present it cannot account for the observed discrepancy.

Another effect of the change in nearest-neighbor (NN) equilibrium positions will be to introduce a new scattering potential, with a range on the order of the NN separation. We have evaluated this "lattice relaxation scattering" using its relation to the electron-phonon interaction. We chose a barrier to represent the scattering potential on the assumption that lattice relaxation scattering should weaken the core potential. If one were to assume that this potential is switched off rapidly when the core hole is annihilated, the change in α_0 would be increased to approximately -0.09. The time scale for this potential change is much longer than for the electronic relaxation, however, and so it should not affect α_0 in the present model. Thus we find no explanation for the experimentally observed lack of mirror symmetry between absorption and emission spectra of simple metals, in particular for the case of Na.

Since one can argue that, e.g., TDOS uncertainties could be the source of the apparent discrepancy between emission and absorption exponents, we feel that it is more important to focus on the comparison of absorption to XPS. If the MND model as stated in Eqs. (1)–(3) was accurate for both absorption and XPS, a common set of phase shifts δ_l would exist which would yield $\alpha=0.22$ and $\alpha_0=0.22$ when inserted into Eqs. (2) and (3). The Friedel sum rule, $\Sigma(2l+1)\delta_l=\pi/2$, is a necessary con-

straint on the phase shifts,[60] and has been translated into exponent compatibility relations.[61,17,12] If one assumes $\alpha=0.22$, the value of α_0 implied by the compatibility relation of Ref. 12 is approximately 0.40; alternatively, if one assumes $\alpha_0=0.22$, then α is required to be 0.15. The differences indicated by these results are far outside experimental uncertainties in the values of α and α_0, which are about 0.02 in both cases. Using the relations of Refs. 61 and 17 the two limits are even more divergent, and we conclude that the XPS and SXA results are incompatible for Na.

We have considered the possibility that phonon coordinate averaging might contribute to this disparity as well. Since the data represent a sampling of all available final configurations, within the Born-Oppenheimer approximation, the local potential is not a fixed quantity. It is apparent from Eqs. (2) and (3) that α_0 and α will be affected differently by such an averaging process, because the δ_l enter their evaluation differently. However, analysis along the lines of Ref. 21 indicates that this effect is insignificant, and SXA and XPS results for Na cannot be reconciled within the MND model.

This result and the spin-orbit ratio of 2 discussed above directly conflict with some conclusions of CWS. In spite of the fact that the Na $L_{2,3}$ absorption spectrum analyzed by CWS contained a sloped background which could lead to a slightly inflated estimate of α_0, we do not understand completely the source of the discrepancy between the present results and those of CWS. It rather appears to us that Ref. 12 represents an attempt to show that the data and the MND model could be made consistent by invoking a "near-edge" criterion. We find no justification for such a criterion in fitting data or in examining the theory, and therefore strongly disagree with CWS regarding Na x-ray thresholds. We also note that a recent Letter by essentially the same workers[20] violated the near-edge criterion, with no apparent justification, in fitting the K edge of Na with a MND line shape. Furthermore, Citrin *et al.*[20] used phase-shift compatibility relations, which were ostensibly firmly established by CWS, to conclude that band narrowing must be invoked in order to achieve an acceptable fit to data. The results which we have presented so far indicate that the support for such compatibility relations is lacking. The dynamical band narrowing[62] should, however, be included in the data analysis, as shown very clearly by the shift between theory and experiment of the van Hove minimum of Na in Fig. 8 of Ref. 32 and Fig. 1 of Ref. 20. To the extent that it can be modeled accurately as a one-electron effect, e.g., a change in the slope of the TDOS or in the position of a van Hove minimum, the band narrowing can be accounted for. Yet a change in the expected TDOS slope of 20% does not alter our primary conclusion, that the MND model fails in its present form to quantitatively describe the Na threshold data. It is therefore necessary to examine the assumptions of the model.

There are physical differences among SXE, SXA, and XPS in Na, due to the short-time behavior of the local potential. In the MND model the infinite-time response function is needed to evaluate the spectra asymptotically near threshold. Though the usual application of the model involves using the infinite-time potential to evaluate the response function, the response function at a given time can be affected by the behavior of the potential at earlier times. While both XPS and absorption involve the promotion of a core electron to an unoccupied state, and important difference between the two spectroscopies lies in the energy of that state, i.e., in the velocity of the active electron. In threshold absorption the relevant speed is near the Fermi velocity, while it is many times that in XPS. In threshold absorption the net initial potential created by the transition is dipolar and weak, and as the active electron is transported away from the core hole the passive electrons can follow the evolving potential, keeping it nearly screened at all times. In XPS the active electron leaves before screening takes place, resulting in a stronger early-time, monopolar potential. In emission the initial potential has already been screened, and decays away after the core hole is annihilated. Thus the transient potential is strongest for XPS, intermediate for SXA, and weakest for SXE, correlating directly with the apparent potential strength needed to describe the three experiments. The question to be answered, then, is to what degree the short-time potential behavior affects quantities like α and α_0.

An early discussion of the bearing of the time dependence of the potential on electron-hole pair (EHP) creation in core spectral measurements was given by Müller-Hartmann *et al.* (MHRT).[63] Their work was later reinterpreted by Gadzuk and Šunjić (GS) in terms of α, the singularity index, the value of which provides a measure of the extent of EHP creation.[64] Plasmon creation caused by a core transition has also been extensively investigated theoretically,[65,66] and the correlation between photoelectron velocity and the plasmon satellite intensity in XPS follows from considerations similar to those of GS. Such satellites have not been observed in absorption, but are well established in SXE.[66] It has long been known[67] that the SXE plasmon satellite intensity is much weaker than the XPS plasmon satellite intensity due to the much slower active electron. The local potential is the same in the case of plasmon generation as for EHP creation, so that an accurate description of the former case should lead to a better understanding of the latter.

The GS result was based on a relatively simple form for the time-dependent potential which is turned on at $t=0, V(t)=V_0(1-e^{\eta t})$ following the work of MHRT, where $\eta \propto v$, the velocity of the photoelectron. They showed that α varies with photoelectron kinetic energy. This by itself implies that there should be a difference between absorption and high-energy XPS. A potential that can describe the XPS and SXE plasmon satellites and which has a similar form is the following:

$$V(t)=V_0(1-e^{-\eta_1 t})+V_1 e^{-\eta_1 t}-V_2 e^{-\eta_2 t},$$

where η_1 characterizes the time dependence of the screening of the core hole by the electron sea and η_2 the velocity of the active electron in XPS or absorption. V_1 serves to approximate the unscreened potential of the core hole, and V_2 the unscreened due to the active elec-

tron. V_0 is the screened potential felt at long times.

We have constrained this model potential by using the dependence of the XPS plasmon satellite intensity on photoelectron velocity.[66] This leads to the values $V_1 \simeq V_2 = 7.5$, $V_0 \simeq 0.5$, $\eta_1 \simeq \omega_p/2\pi$, and $\eta_2 = 0.37v/\lambda$, where λ is the Thomas-Fermi screening length. These values yield a plasmon satellite intensity of about 50% of the Na main line at high velocity, and 4% for $v = v_F$ reproducing the results of Ref. 66. GS have established that the terms containing V_0 are sufficient to show significant effects on EHP creation due to changes in photoelectron velocity in XPS, and their result has received experimental support.[68] Since the additional terms involving V_1 and V_2 are so much larger, and vary with the electron velocity much as GS assumed, we suggest that these terms, which are necessary to explain the plasmon satellites, are also responsible for the incompatibility of the threshold exponents between XPS and absorption. Unfortunately, it is not simple to extend the GS result to the more complicated potential given above, and further theoretical work studying the time-dependent aspects of this problem will be necessary to quantitatively test this assertion.

In the MND model a potential with a simple dependence on the spatial coordinate (r) representing the presence of the core hole is turned on at $t=0$. We have argued here that this potential depends significantly on the time and weakly on the NN distance R. We can express this as $V = V(r,R,t)$. Each of the three experiments discussed above then has its "own potential." In emission the transient early-time potential is different from that for absorption, and any lattice relaxation that occurs changes the potential even further from that for absorption. In the case of XPS the time dependence is different from that for either absorption or emission. Our results indicate that the infinite-time response function is different for each of the three experiments. The power-law model remains a good description of the spectra and is able to describe the data in an accessible energy range near threshold. However, whenever the R and t dependence of V are significant, the use of a compatibility relation with a single set of phase shifts to relate one experiment to another will fail.

V. SUMMARY

We have investigated the differences in line shape among the three absorption spectral functions. $\mathrm{Im}(-1/\epsilon)$, μ, and ϵ_2, and found that they are quite significant at the k $M_{2,3}$ edge, but negligible at the Na $L_{2,3}$ threshold. We predict that the outer p-core absorption of Rb and Cs will follow a pattern similar to that of K in this regard. We have compared the Na $L_{2,3}$ data of Haensel *et al.*[31] with Na IES data, and find consistent exponent values. The spin-orbit ratio of 1.95 ± 0.10 for all the cases we have studied[43] of the Na $L_{2,3}$ spectrum indicates that exchange mixing is not significant in the Na $L_{2,3}$ data, in agreement with an earlier analysis.[17] We have used an improved line-shape fitting function, and have confirmed the results of Slusky *et al.*[17] with the exception that our estimate of lifetime broadening is significantly lower. The lack of mirror symmetry between emission and absorption edges of Na and K has also been confirmed by the present results, and asymmetric broadening due to partial phonon relaxation has been ruled out as a viable cause. The effect of the surface core-level binding-energy shift on line-shape analysis of Na XPS data has been investigated, and the asymmetry parameter does not appear to be very sensitive to that factor.

We therefore empirically support the view that the line-shape parameters extracted from the different Na x-ray core spectra are incompatible within the MND framework. We propose that previously unconsidered dynamical effects are the most likely cause of this incompatibility, and that the MND model should be extended to include them.

ACKNOWLEDGMENTS

We gratefully acknowledge VAX computer time generously provided by J. McCarthy, valuable conversations with E. Jensen, and helpful discussions with other members of our research group, P. Livins, R. Carson, D. Husk, J. Nithianandam, and S. Velasquez, with special thanks to C. Tarrio for help in analyzing the IES data. This research was supported in part by National Science Foundation Grant No. DMR85-15684.

*Present address: Physics Dept., Univ. of Pennsylvania, c/o Bldg. 725, NSLS/U12, Brookhaven National Laboratory, Upton, NY 11973-5000.

[1]H. W. B. Skinner, Philos. Trans. R. Soc. London, Ser. A **239**, 95 (1940)

[2]W. M. Cady and D. H. Tomboulian, Phys. Rev. **59**, 389 (1941).

[3]P. T. Landsberg, Proc. R. Soc. London Ser. A **62**, 806 (1949).

[4]J. Pirenne and P. Longe, Physica **30**, 277 (1964).

[5]P. Livins and S. E. Schnatterly, Phys. Rev. B **37**, 6731 (1988).

[6]P. Livins, Ph.D. thesis, University of Virginia, Charlottesville, 1988 (unpublished).

[7]G. D. Mahan, Phys. Rev. **163**, 612 (1967).

[8]P. W. Anderson, Phys. Rev. Lett. **18**, 1049 (1967).

[9]P. Nozières and C. T. De Dominicis, Phys. Rev. **178**, 1097 (1969).

[10]For a comprehensive review, see C.-O. Almbladh and L. Hedin, in *Handbook on Synchrotron Radiation*, edited by E. E. Koch (North-Holland, New York, 1983), Vol. 1B, p. 607.

[11]U. von Barth and G. Grossmann, Phys. Scr. **28**, 107 (1983).

[12]P. H. Citrin, G. K. Wertheim, and M. Schlüter, Phys. Rev. B **20**, 3067 (1979).

[13]S. Doniach and M. Šunjić, J. Phys. C **3**, 285 (1970).

[14]C. P. Flynn, Phys. Rev. Lett. **37**, 1445 (1976), and references therein.

[15]P. H. Citrin, G. K. Wertheim, and Y. Baer, Phys. Rev. B **16**, 4526 (1977), and references therein.

[16]R. P. Gupta and A. J. Freeman, Phys. Lett. A **59**, 223 (1976).

[17]S. E. G. Slusky, S. E. Schnatterly, and P. C. Gibbons, Phys. Rev. B **20**, 379 (1979).

[18]C. A. Swarts, J. D. Dow, and C. P. Flynn, Phys. Rev. Lett. **43**, **21**, 4552 (1980). We note that Callcott, Arakawa, and Ederer (Ref. 32) obtained an L_3/L_2 intensity ratio of 2.7 using SXA,

158 (1979).
[19]U. von Barth and G. Grossmann, Phys. Rev. B **25**, 5150 (1982).
[20]P. H. Citrin, G. K. Wertheim, T. Hashizume, F. Sette, A. A. MacDowell, and F. Comin, Phys. Rev. Lett. **61**, 1021 (1988).
[21]P. A. Bruhwiler, P. Livins, and S. E. Schnatterly, Phys. Rev. B **39**, 5480 (1989).
[22]T. T. Rantala, Phys. Rev. B **28**, 3182 (1983).
[23]S. E. Schnatterly, in *Solid State Physics,* edited by H. Ehrenreich, F. Seitz, and D. Turnbull (Academic, New York, 1979), Vol. 34, p. 275.
[24]G. D. Mahan, Phys. Rev. B **15**, 4587 (1977).
[25]C.-O. Almbladh, Phys. Rev. B **16**, 4343 (1977).
[26]P. A. Bruhwiler and S. E. Schnatterly, Phys. Rev. Lett. **61**, 357 (1988).
[27]R. Kammerer, J. Barth, F. Gerken, C. Kunz, S. A. Flodstrøm, and L. I. Johansson, Phys. Rev. B **26**, 3491 (1982).
[28]R. L. Fink, P. N. First, and C. P. Flynn, Phys. Rev. B **38**, 5839 (1988).
[29]P. H. Citrin, G. K. Wertheim, and Y. Baer, Phys. Rev. B **27**, 3160 (1983).
[30]P. Livins, T. Aton, and S. E. Schnatterly, Phys. Rev. B **38**, 5511 (1988).
[31]R. Haensel, G. Keitel, P. Schreiber, B. Sonntag, and C. Kunz, Phys. Rev. Lett. **23**, 528 (1969).
[32]T. A. Callcott, E. T. Arakawa, and D. L. Ederer, Phys. Rev. B **18**, 6622 (1978).
[33]S. Sato, T. Miyahara, T. Hanyu, S. Yamaguchi, and T. Ishii, J. Phys. Soc. Jpn. **47**, 836 (1979).
[34]T. Ishii, Y. Sakisaka, S. Yamaguchi, T. Hanyu, and H. Ishii, J. Phys. Soc. Jpn. **42**, 876 (1977).
[35]C.-O. Almbladh, A. L. Morales, and G. Grossmann, Phys. Rev. B **39**, 3489 (1989).
[36]P. A. Bruhwiler, Ph.D. thesis, University of Virginia, Charlottesville, 1988 (unpublished).
[37]C.-O. Almbladh and P. Minnhagen, Phys. Status Solidi B **85**, 135 (1978).
[38]F. A. Zhivopistsev and F. E. Comas, Vest. Mosk. Univ. Fiz. **36**, 20 (1981) [Moscow Univ. Phys. Bull. **36**, 23 (1981)].
[39]K. Ohtaka and Y. Tanabe, Phys. Rev. B **30**, 4235 (1984).
[40]Y. Onodera, J. Phys. Soc. Jpn. **39**, 1482 (1975).
[41]R. S. Crisp, Philos. Mag. **36**, 609 (1977). A comment on the general applicability of the present theory of exchange mixing at *p*-core thresholds seems appropriate at this point. The fact that the $p_{3/2}/p_{1/2}$ intensity ratio varies from ~ 1.2, ~ 1.7, ~ 1.7, and ~ 2.0 in atomic Na [H. W. Wolff, K. Radler, B. Sonntag, and R. Haensel, Z. Phys. **257**, 353 (1972)], K [H. Beutler and K. Guggenheimer, *ibid.* **87**, 188 (1933)], Rb [H. Beutler, *ibid.* **91**, 131 (1934)], and Cs [H. Beutler and K. Guggenheimer, *ibid.* **88**, 25 (1934)], respectively, to ~ 2.0, ~ 2.4 (the present work and Ref. 17), and with less certainty > 2 and > 2 (based on a visual inspection of the data in Refs. 33 and 34) for the same series in the solid, respectively, indicates that the spectra in the solids are not described merely by screening of the atomic exchange interaction, as postulated by Onodera, except perhaps for Na. While it is possible that this is simply an effect of the potential near the core [see, e.g., the work of G. W. Bryant, Phys. Rev. B **19**, 2801 (1979)], it represents a gap in our understanding at present. Nevertheless, for the sake of completeness and because Onodera's result was emphasized in Ref. 12, we will discuss exchange mixing extensively for the case of Na.
[42]T. Kita, J. Phys. Soc. Jpn. **56**, 4598 (1987).
[43]J. A. Tagle, E. T. Arakawa, and T. A. Callcott, Phys. Rev. B in marked disagreement with the present analysis of the IES data of Ref. 17 and the SXA data of Haensel *et al.* (Ref. 31). The higher value of this ratio obtained in Ref. 32 could be due to the presence of pinholes in the Na film used in the SXA measurments. In contrast, IES measurements are not susceptible to pinholes (see Ref. 23). Yet a back-of-the-envelope analysis indicates, e.g., that a 5000-Å-thick sample would need to consist of approximately 40% pinholes for this to be the sole source of the difference in the measured ratio, which seems excessive. However, we believe that our results are accurate, and take the good agreement with the data of Ref. 31 as strong support for their reliability.
[44]T. Miyahara, S. Sato, T. Hanyu, A. Kakizaki, S. Yamaguchi, and T. Ishii, J. Phys. Soc. Jpn. **49**, 194 (1980).
[45]R. S. Crisp, J. Phys. F **10**, 511 (1980).
[46]P. N. First, R. L. Fink, and C. P. Flynn, J. Phys. F **17**, L29 (1987).
[47]R. S. Crisp, J. Phys. F **13**, 1325 (1983).
[48]A. Mansour and S. E. Schnatterly, Phys. Rev. Lett. **59**, 567 (1987).
[49]T. A. Callcott, E. T. Arakawa, and D. L. Ederer, Phys. Rev. B **16**, 5185 (1977).
[50]A. Mansour, Ph.D. thesis, University of Virginia, Charlottesville, 1987 (unpublished) presents an analysis of the data of Ref. 50 in terms of the model of Ref. 49, with excellent results.
[51]See, e.g., D. B. Fitchen, in *Physics of Color Centers,* edited by W. B. Fowler (Academic, New York, 1968), p. 293.
[52]C.-O. Almbladh and A. L. Morales, J. Phys. F **15**, 991 (1985).
[53]H. R. Schober and P. H. Dederichs, in *Landolt-Börnstein: Numerical Data and Functional Relationships in Science in Technology,* edited by K.-H. Hellwege and J. L. Olsen (Springer-Verlag, New York, 1981), Ser. 3, Vol. 13a.
[54]T. A. Callcott and D. L. Ederer, private communication.
[55]U. Fano, Phys. Rev. **124**, 1866 (1961).
[56]T. Kita, K. Ohtaka, and Y. Tanabe, J. Phys. Soc. Jpn. **56**, 4609 (1987).
[57]P. N. First, private communication.
[58]M. Cardona and L. Ley, in *Photoemission in Solids I,* edited by M. Cardona and L. Ley (Springer-Verlag, New York, 1978), p. 265.
[59]D. A. Papaconstantopoulos, *Handbook of the Band Structure of Elemental Solids* (Plenum, New York, 1986).
[60]N. H. March, in *Band Structure Spectroscopy of Metals and Alloys,* edited by D. J. Fabian and L. M. Watson (Academic, New York, 1973), p. 297.
[61]J. D. Dow, J. E. Robinson, J. H. Slowik, and B. F. Sonntag, Phys. Rev. B **10**, 432 (1974).
[62]I.-W. Lyo and E. W. Plummer, Phys. Rev. Lett. **60**, 1558 (1988); B. S. Itchkawitz, I.-W. Lyo, and E. W. Plummer, *ibid.* (to be published).
[63]E. Müller-Hartmann, T. V. Ramakrishnan, and G. Toulouse, Phys. Rev. B **3**, 1102 (1971).
[64]J. W. Gadzuk and M. Šunjić, Phys. Rev. B **12**, 524 (1975).
[65]J. E. Inglesfield, J. Phys. C **16**, 403 (1983), and references therein.
[66]P. Livins and S. E. Schnatterly, Phys. Rev. B **37**, 6742 (1988), and references therein.
[67]D. C. Langreth, Phys. Rev. Lett. **26**, 1229 (1971). Similar effects have recently been involved to explain the band narrowing in photoemission; see A. Nakano and S. Ichimaru, Phys. Rev. B **39**, 4938 (1989).
[68]F. J. Himpsel, D. E. Eastman, and E. E. Koch, Phys. Rev. Lett. **44**, 214 (1980).